

# Dynamic scaling in natural swarms

Andrea Cavagna<sup>1\*</sup>, Daniele Conti<sup>2</sup>, Chiara Creato<sup>1,2</sup>, Lorenzo Del Castello<sup>1,2</sup>, Irene Giardina<sup>1,2,3</sup>, Tomas S. Grigera<sup>4,5</sup>, Stefania Melillo<sup>1,2\*</sup>, Leonardo Parisi<sup>1,6</sup> and Massimiliano Viale<sup>1,2</sup>

**Collective behaviour in biological systems presents theoretical challenges beyond the borders of classical statistical physics. The lack of concepts such as scaling and renormalization is particularly problematic, as it forces us to negotiate details whose relevance is often hard to assess. In an attempt to improve this situation, we present here experimental evidence of the emergence of dynamic scaling laws in natural swarms of midges. We find that spatio-temporal correlation functions in different swarms can be rescaled by using a single characteristic time, which grows with the correlation length with a dynamical critical exponent  $z \approx 1$ , a value not found in any other standard statistical model. To check whether out-of-equilibrium effects may be responsible for this anomalous exponent, we run simulations of the simplest model of self-propelled particles and find  $z \approx 2$ , suggesting that natural swarms belong to a novel dynamic universality class. This conclusion is strengthened by experimental evidence of the presence of non-dissipative modes in the relaxation, indicating that previously overlooked inertial effects are needed to describe swarm dynamics. The absence of a purely dissipative regime suggests that natural swarms undergo a near-critical censorship of hydrodynamics.**

Scaling is one of the most powerful concepts in statistical physics. At the static level, the essential idea of the scaling hypothesis is that the only natural length scale of a system close to its critical point is the correlation length,  $\xi$ . In general, one could expect the behaviour of a system to depend in complicated ways on the parameters controlling its vicinity to the critical point. The scaling hypothesis states that the situation is in fact simpler: the correlation functions depend on all these control parameters only through  $\xi$  (refs 1,2). The dynamic scaling hypothesis pushes this idea a step further by establishing a connection between space and time<sup>3,4</sup>: when the correlation length is large, both the characteristic timescale and the dynamic correlation function depend on the control parameters only through the correlation length, which therefore becomes the sole relevant scale of the system also at the dynamical level. The dynamic scaling hypothesis is rooted in the renormalization group idea of studying how the laws of nature change under a rescaling of space and time. Close to criticality, scale invariance guarantees that all inessential microscopic details drop out of the quantitative description of a system. This is universality, the fundamental reason why a handful of physical laws have a vast range of applicability, from condensed matter to particle physics<sup>5,6</sup>.

The key ingredient of scaling is the existence of a large correlation length, namely much larger than the microscopic length scales of the system. This is not an exclusive prerogative of statistical physics. Strong correlations are found in many biological systems; indeed, the very existence of significant correlations is arguably the best definition of collective behaviour<sup>7</sup>. Bird flocks<sup>8</sup>, fish schools<sup>9</sup>, mammal herds<sup>10</sup>, insect swarms<sup>7</sup>, bacterial clusters<sup>11,12</sup> and proteins<sup>13</sup> are all biological systems where static correlations have been found to be strong. One may then ask whether the concepts of scaling and universality make any sense in these contexts too. Even though the complexity of biological systems may make us coy about this kind of question, one should remember that even in statistical physics scaling is not a rigorous theorem, but rather

a phenomenological conjecture about what is relevant and what is not in a strongly correlated system. The only key assumption at the basis of scaling is that the correlation length is much larger than all microscopic scales. Hence, before banning scaling from the living world, one should test it experimentally. Here we investigate the dynamic scaling hypothesis in natural swarms of insects. We find that experimental data are consistent with scaling and that a seemingly new dynamical universality class emerges.

By using multi-camera techniques<sup>14</sup>, we reconstruct individual three-dimensional (3D) trajectories in swarms of midges in their natural environment (Diptera: Chironomidae and Diptera: Ceratopogonidae; Fig. 1 and Methods). To perform a dynamic analysis, we conducted a new data-taking campaign based on the experimental set-up of ref. 7, reaching a total of 30 natural swarms of various sizes and densities (Supplementary Table 1). After the pioneering works of refs 15–17, new generation experiments on swarms have been performed both in the laboratory<sup>18,19</sup>, and in the wild<sup>7,20–22</sup>. From the trajectories, we compute the spatio-temporal correlation function of the velocity fluctuations in the Fourier space of the wavenumber  $k$ ,

$$C(k, t) = \left\langle \frac{1}{N} \sum_{ij} \frac{\sin[kr_{ij}(t_0, t)]}{kr_{ij}(t_0, t)} \delta \hat{v}_i(t_0) \cdot \delta \hat{v}_j(t_0 + t) \right\rangle$$

where  $\delta \hat{v}_i$  is the dimensionless velocity fluctuation of insect  $i$  (see Methods) and the brackets indicate an average over the earlier time  $t_0$ ; the distance between insects  $i$  and  $j$  at different times is  $r_{ij}(t_0, t) = |\mathbf{r}_i(t_0) - \mathbf{r}_j(t_0 + t)|$ , where positions are calculated in the centre-of-mass reference frame (see Methods).  $C(r, t)$ , the real-space counterpart of  $C(k, t)$ , measures to what extent the velocity change of an insect at time  $t_0$  is similar to that of another insect at distance  $r$  and at a later time  $t_0 + t$  (Fig. 1c). For a frequency analysis of laboratory swarm dynamics, see refs 23,24.

The correlation function depends on time,  $t$ , on wavenumber,  $k$ , and very likely on other factors determining the behaviour of

<sup>1</sup>Istituto Sistemi Complessi, Consiglio Nazionale delle Ricerche, UOS Sapienza, 00185 Rome, Italy. <sup>2</sup>Dipartimento di Fisica, Università Sapienza, 00185 Rome, Italy. <sup>3</sup>INFN, Unità di Roma 1, 00185 Rome, Italy. <sup>4</sup>Instituto de Física de Líquidos y Sistemas Biológicos CONICET - Universidad Nacional de La Plata, B1900BTE La Plata, Argentina. <sup>5</sup>CCT CONICET La Plata, Consejo Nacional de Investigaciones Científicas y Técnicas, B1900BTE La Plata, Argentina. <sup>6</sup>Dipartimento di Informatica, Università Sapienza, 00198 Rome, Italy. \*e-mail: [andrea.cavagna@roma1.infn.it](mailto:andrea.cavagna@roma1.infn.it); [stefania.melillo@cnr.it](mailto:stefania.melillo@cnr.it)

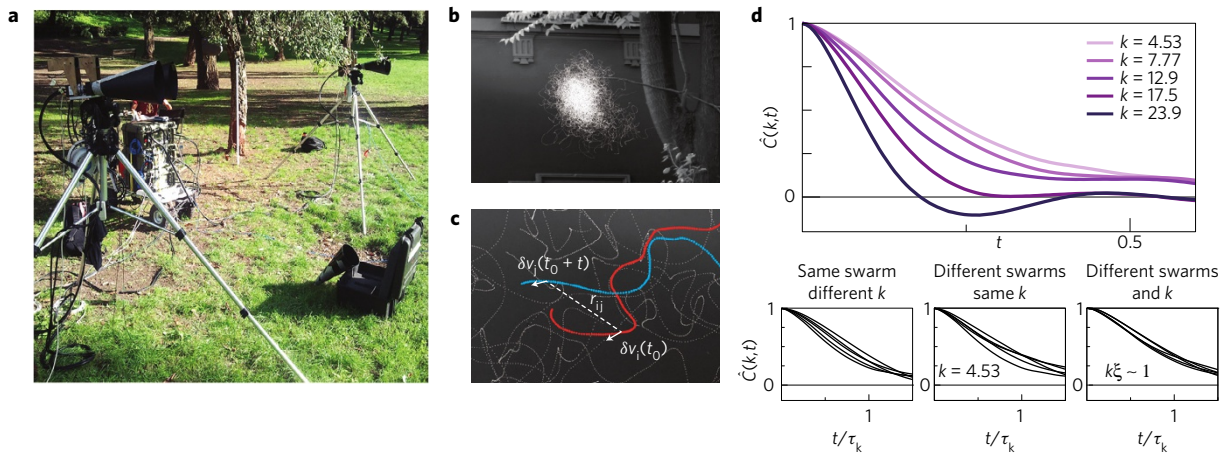


**Figure 1 | Experiment and temporal correlation.** **a**, A system of three synchronized high-speed cameras shooting at 170 fps is used to collect video sequences of midge swarms in their natural environment. **b**, A swarm of approximately 300 midges. **c**, Close-up of two trajectories within the swarm. **d**, Upper panel: normalized correlation function  $\hat{C}(k, t)$  in one natural swarm at various values of  $k$ . Bottom panels: correlation as a function of the rescaled time,  $t/\tau_k$ , in various attempts to rescale the data (see text).

swarms. Can we reduce this complexity? In Fig. 1d we report the normalized correlation,  $\hat{C}(k, t) \equiv C(k, t)/C(k, t=0)$ , as a function of time, for different values of  $k$ , in the same swarm. We observe that the temporal decay rate of the correlation,  $\tau_k$ , strongly depends on  $k$  (see Methods and Supplementary Appendix A for the definition of  $\tau_k$ ). A naive guess is that the correlation depends on  $k$  only through its timescale, in which case  $\hat{C}$  versus  $t/\tau_k$  at various  $k$  should collapse onto the same curve. The data show that this is not the case (Fig. 1d, bottom panels): not only the timescale, but also the shape of the correlation function, depends on the wavenumber. Moreover, Fig. 1d shows that at fixed  $k$  the correlation as a function of  $t/\tau_k$  is different from swarm to swarm. We conclude that the shape of  $\hat{C}(t/\tau_k)$  depends explicitly both on  $k$  and on the set of biological and environmental parameters controlling the swarms' dynamics,  $\mathbf{P} = (p_1, p_2, \dots)$ , so that  $\hat{C} = \hat{C}(t/\tau_k; k, \mathbf{P})$ . Dynamical correlations in swarms seem not to scale with anything and to depend on everything.

Our failed attempts to separately rescale the dependence on the wavenumber  $k$  and on the unknown factors  $\mathbf{P}$  leaves open the possibility to rescale them simultaneously, namely that the correlation is a function of some dimensionless combination of  $k$  and  $\mathbf{P}$ .  $k$  has the dimensions of an inverse length; hence, we need to multiply it by some natural length scale that depends on  $\mathbf{P}$ . Such length scale must be intrinsic to the swarm and experimentally accessible, requirements that narrowly restrict the choice. A possible candidate is the correlation length,  $\xi$ , which can be computed in each swarm directly from the data (see ref. 7 and Methods) and is known to depend on the external factors (certainly density and size, as shown in ref. 22). We can now hypothesize that the product  $k\xi(\mathbf{P})$  exhausts all dependence on  $k$  and on  $\mathbf{P}$  of the correlation, namely that  $\hat{C}(t/\tau_k; k, \mathbf{P}) = \hat{C}(t/\tau_k; k\xi(\mathbf{P}))$ . If this is true, by fixing the product  $k\xi$  we should eliminate both the dependence on  $k$  and on  $\mathbf{P}$ . The simplest way to fix the product  $k\xi$  in our data is to select  $k = 1/\xi$  in each swarm:

$$\hat{C} = \hat{C}(t/\tau_k, 1) \quad (1)$$

We test this hypothesis in Fig. 1d: data show that the spread of the correlation functions among different swarms is now reduced, which seems a promising step forward in terms of simplification of the data complexity. Is there a theoretical framework within which we can interpret and perhaps improve this result?

Natural swarms have a correlation length  $\xi$  that is large compared with the interparticle distance and a susceptibility that

far exceeds that of a non-interacting system<sup>7,22</sup>. These are the essential prerequisites of dynamical scaling; hence, it is tempting to interpret the results above in terms of this framework. The dynamic scaling hypothesis<sup>3,4,25,26</sup> states that the temporal correlation and its characteristic time are homogeneous functions of  $k$  and  $\xi$  and that the dependence on the control parameters  $\mathbf{P}$  runs only through  $\xi$ ,

$$\hat{C}(k, t, \mathbf{P}) = \hat{C}(t/\tau_k; k\xi(\mathbf{P})) \quad (2)$$

$$\tau_k = k^{-z} g(k\xi(\mathbf{P})) \quad (3)$$

where  $g$  is an unknown scaling function. The fact that everything depends on the product  $k\xi$  means that the correlation length is the only quantity needed to locate a system in its parameters space. Equation (3) embodies the renormalization group idea that to a rescaling of space,  $x \rightarrow x/b$ , corresponds a rescaling of time,  $t \rightarrow t/b^z$ , a balance regulated by the so-called dynamical critical exponent,  $z$  (ref. 27), see Supplementary Appendix A. The dynamical scaling relation (2) is consistent with Fig. 1d. However, (3) says something more, namely that if we move along paths of constant  $k\xi$  the characteristic time becomes a power law,

$$\tau_k \sim k^{-z} \quad (4)$$

so that we can rescale time directly with a power of  $k$ , finally giving

$$\hat{C} = \hat{C}(k^z t, 1) \quad (5)$$

We tested relation (5) and found a very good collapse of the data when  $z = 1.2$  (Fig. 2b). This scaling is the most compelling of those we tried, indicating that the dynamic scaling hypothesis (see Supplementary Appendix A) is the most effective way to reduce the complexity of the correlation. Moreover, we find that the characteristic time scales with  $k$  in accordance with equation (4): although the scatter is significant, the plot shows a clear correlation between  $\log \tau_k$  and  $\log k$  ( $P$ -value  $\sim 10^{-6}$ , Fig. 2c), with exponent  $z = 1.12 \pm 0.16$ , consistent with the value of  $z$  from the collapse. Given the limited range of lengths and times, a fit to (4) is not the safest way to determine  $z$ . On the other hand, to collapse the correlation functions via relation (5) we do not need to compute the characteristic time,  $\tau_k$ ; hence, this is a far cleaner determination of the critical exponent  $z$ . In Supplementary Fig. 2 we show how dramatically worse the collapse looks like when we try to scale the correlations via a different exponent.

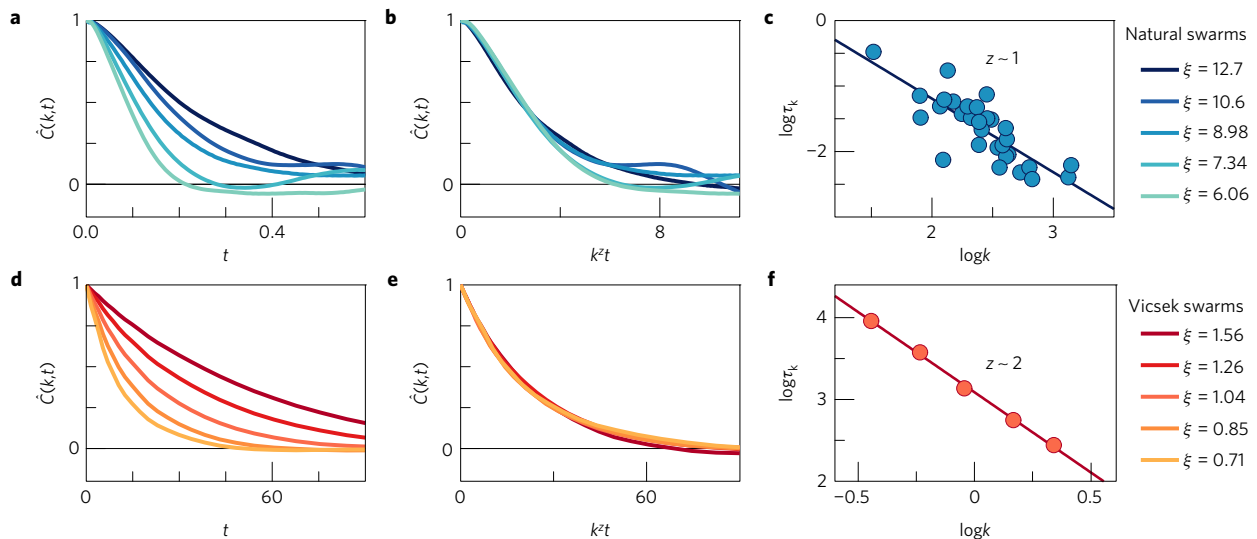


**Figure 2 | Dynamic scaling and critical exponent.** **a**, Normalized time correlation function,  $\hat{C}(k, t)$ , evaluated at  $k = 1/\xi$ , in several natural swarms. Sizes range from  $N = 100$  to  $N = 300$ , time is measured in seconds and correlation length  $\xi$  is centimetres. **b**,  $\hat{C}(k, t)$  as a function of the scaling variable  $k^2 t$  for the same events as in **a**;  $z = 1.2$  gives the optimal collapse of the curves according to equation (5). The quality of the collapse deteriorates for longer times because  $\hat{C}(k, t)$  is the average over  $t_{\max} - t$  time pairs ( $t_{\max}$  is the sequence duration); hence, large  $t$  data are noisier. **c**, Characteristic timescale,  $\tau_k$ , computed at  $k = 1/\xi$ , as a function of  $k$  (log-log scale). Each point corresponds to a different natural swarm; all experimental events are reported.  $P$  value  $= 10^{-6}$ ,  $z = 1.12 \pm 0.16$ , consistent with the estimate from the collapse in **b**. **d–f**, Dynamic scaling analysis of the 3D Vicsek model for  $N = 128, 256, 512, 1,024, 2,048$  particles;  $\tau_k$  scale with  $k$  with an exponent  $z = 1.96 \pm 0.04$ , which also produces an excellent collapse of the correlation functions.

If we plug  $k = 1/\xi$  into (4) we obtain,

$$\tau_k \sim \xi^z \quad (6)$$

Natural swarms seem therefore to conform to a fundamental law of statistical physics: systems that are more spatially correlated (larger correlation length  $\xi$ ) are also more temporally correlated (larger characteristic time  $\tau_k$ ). This is the core of the dynamic scaling hypothesis: in a strongly correlated system, space and time are connected to each other by the exponent  $z$ . The fact that dynamic scaling is consistent with experiments on natural swarms seems to us noteworthy, because swarms' collective behaviour is determined by at least two control parameters (noise level and density<sup>22</sup>), plus potentially many other biological and environmental factors we are unaware of; yet the correlation function appears to be ruled by just one quantity, the correlation length. This fact strongly supports the idea that  $\xi$  alone contains the most important effects of the fluctuations<sup>26</sup>. The growth of the relaxation time with the correlation length, equation (6), also opens intriguing possibilities about the off-equilibrium formation of topological defects in strongly correlated biological systems under fast quenches, a phenomenon known as the Kibble–Zurek mechanisms<sup>28,29</sup>. Note, though, that the near-criticality and scale-free nature of swarms found in ref. 22, namely the fact that the correlation length scales with the system's size, is not a necessary assumption of the scaling hypothesis; to satisfy scaling one simply needs  $\xi$  to be much larger than the microscopic scales, a far weaker condition that is certainly satisfied in natural swarms<sup>7</sup>.

Given the non-standard statistical nature of the system under investigation, classic dynamical scaling is not the only possible interpretation of our data. One could envisage other, more biologically related mechanisms giving rise to the same collapse of the data. However, the experimental evidence that the correlation is simply a function of the product  $k\xi$  and therefore that all (or most) of the external factors are encapsulated into a single quantity,  $\xi$ , is independent of any theoretical scheme and it rests as a hard fact other interpretations must confront.

The value of  $z$  determines the dynamic universality class of the system and it is therefore instructive to compare natural

swarms ( $z \approx 1$ ) with known theoretical models. The classic Heisenberg model of ferromagnetic alignment (Model A in the Halperin–Hohenberg classification<sup>27</sup>) has  $z \approx 2$ ; other non-dissipative models as Model G and Model J have  $z = 3/2$  and  $z = 5/2$ , respectively<sup>27</sup>. However, these are equilibrium lattice models that completely fail to describe the self-propelled nature of real swarms. A minimal step towards incorporating the effects of self-propulsion is the Vicsek model<sup>30</sup> (see Methods). This model has been originally introduced to describe the collective behaviour of flocks, namely an ordered phase in which velocities are aligned. Yet the Vicsek model has been studied also close to its ordering transition, where the polarization is low<sup>31–33</sup>; in this disordered phase the phenomenology of the Vicsek model is similar to that of swarms, in that the equal time velocity–velocity correlation functions are the same and the Vicsek susceptibility and correlation length depends on density as in natural swarms<sup>7,22</sup>. Of course, the Vicsek model is far from being realistic and its lack of cohesion forces one to simulate the model with periodic boundary conditions, which is as unrealistic in flocks as in swarms. More realistic models certainly exist<sup>34,35</sup>; hence, we study the Vicsek model merely as a benchmark for the dynamics, a stepping stone between equilibrium lattice models and biologically realistic models of swarms. The dynamic critical exponent of the Vicsek model near the ordering transition has been computed numerically in ref. 32 in  $d = 2$ , where it has been found  $z \approx 1.3$ . On the other hand, in the ordered phase the hydrodynamic theory of flocking<sup>36,37</sup> predicts  $z = 2(d + 1)/5$ , namely  $z = 1.6$  in three dimensions, consistently with numerical simulations<sup>38</sup>. Hence, no estimate of  $z$  exists in the literature for the Vicsek model in  $d = 3$  and in the swarm (disordered) phase. We run simulations of this case and find that the 3D Vicsek model in its near-critical paramagnetic phase satisfies dynamic scaling remarkably well (Fig. 2d–f; see Methods for details of the simulation). Both the collapse of the time correlations and the scaling of  $\tau_k$  with  $k$  give the dynamic critical exponent  $z = 1.96 \pm 0.04$ , practically the same as the classical Heisenberg model; this may be due to the fact that self-propulsion effects are not strong enough to change the equilibrium value of  $z$ , or it could be that corrections to  $z$  kick in at sizes much larger than those of natural swarms. We are not aware of other estimates of  $z$  in



models of swarm behaviour. The discrepancy between the dynamic critical exponent of natural swarms and that of all other 3D models, both on- and off-lattice, suggests that natural swarms belong to a potentially novel dynamic universality class. This opens intriguing new alleys for theoretical investigation.

A further hint that there is something qualitatively new in the dynamics of natural swarms comes from the shape of the time correlation function. While the Vicsek model displays the classic exponential relaxation of dissipative statistical models, real swarms have a clearly non-exponential correlation function, characterized by a vanishing first derivative for  $t < \tau_k$  (Fig. 3a). This feature seems at odds with the disordered nature of swarms and the seemingly dissipative motion of midges, both suggesting a purely diffusive dynamics of the velocity fluctuations, and thus exponential relaxation. A concave correlation for  $t < \tau_k$ , on the other hand, is reminiscent of non-dissipative inertial phenomena<sup>39</sup>. It is therefore important to accurately verify this empirical result. To this aim we define the function

$$h(x) \equiv -\frac{1}{x} \log \hat{C}(x), \quad x \equiv t/\tau_k \quad (7)$$

and study it in the interval  $x \in [0, 1]$ , that is, for times  $t < \tau_k$ . For purely exponential relaxation  $h(x) \rightarrow 1$  for  $x \rightarrow 0$ , while a flat time correlation gives  $h(x) \rightarrow 0$ . We computed  $h(x)$  in all swarms and find a clear difference between natural and Vicsek swarms (Fig. 3), with the former showing a significantly lower value of  $h(x)$ . We remark that this phenomenon emerges in the whole interval  $t < \tau_k$ , not for unnaturally short timescales.

A vanishing first derivative of the time correlation function can only arise if the dynamical propagator has two or more poles in the complex plane of the frequency (see Supplementary Appendix B for proof), namely if the dispersion polynomial is of degree two or larger. This is an indication that the dynamical equations of the system must involve time derivatives of the second order (or higher), which we may call inertial terms. In fact, we can say more: if inertia were present, but dissipation were large compared with it, the flat form of the correlation would be restricted to  $t \ll \tau_k$ ; hence, it could not be observed experimentally; hence, the evidence of a flat correlation for  $t \sim \tau_k$  not only implies that inertial terms exist, but also that they are relevant, namely that the dynamics over the experimental timescales is not purely dissipative (see refs 39,40 and Supplementary Appendix C). The fact that we observe non-dissipative modes in the velocity correlation suggests that second-order inertial terms are directly present in the dynamic equations for  $\mathbf{v}_i$ , as it happens in real flocks<sup>27,41</sup>. However, it could also be that non-dissipative relaxation is the result of a coupling between density waves and velocity fluctuations, similar to what happens in the Toner–Tu theory of flocking<sup>36</sup>. Even though the purely exponential relaxation we find in Vicsek swarms makes the second hypothesis less likely, it is hard to make a call purely based on our data. To make progress it would be crucial to repeat our analysis in swarm models more realistic and detailed than Vicsek<sup>34,42</sup>.

The evidence of non-dissipative modes may seem surprising, as one would expect all such modes to be damped in a system lacking spontaneous order, as is the case of swarms. Actually, the fate of non-dissipative modes in the disordered phase of a system depends on the product  $k\xi$  (ref. 26): in the so-called hydrodynamic regime,  $k\xi \ll 1$ , we are probing length scales much larger than the correlation length, so that all excitations are deeply damped and relaxation is exponential. But if  $k\xi \sim 1$ , as in our data, we are probing scales within a single correlated region, so that fluctuations invalidate the long-wavelength assumption of hydrodynamics. By far the most conspicuous hallmark of the failure of hydrodynamics in the  $k\xi \sim 1$  regime is the emergence of non-dissipative propagating modes even in the disordered phase<sup>26,43,44</sup>. The consequence of this phenomenon in the time domain is a temporal correlation

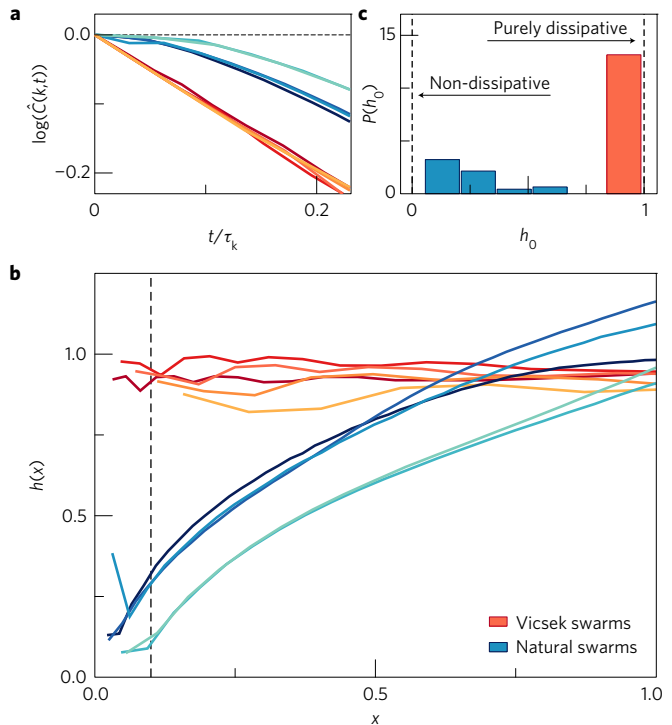


**Figure 3 | Non-dissipative relaxation.** **a**, The correlation in Vicsek swarms displays exponential relaxation (linear decay in semi-log scale), while natural swarms have a strongly non-exponential correlation function (flat derivative for small  $t$ ). **b**, To quantify the different form of the correlation we calculate the function  $h(x)$  defined in (7), where  $x = t/\tau_k$ ; in contrast with Vicsek, natural swarms are characterized by a small value of  $h(x)$  in the interval  $0 < t < \tau_k$ . **c**, We compute the intercept  $h_0 = h(x=0.1)$  for all data and report its distribution: all natural swarms have a low first derivative, indicating the existence of non-dissipative modes, while Vicsek swarms have a purely dissipative peak at  $h_0 \sim 1$ .

function with flat first derivative, which is indeed what we find in natural swarms.

It is intriguing to interpret our experimental results in terms of non-dissipative magnetic materials<sup>26</sup> and superfluids<sup>27</sup>, which are characterized in their ordered phase by propagation of the fluctuations of the order parameter, namely by spin waves<sup>40</sup>. Such propagating modes are also found in polarized animal groups, such as flocks, where they guarantee swift transmission of the velocity changes, allowing the group to maintain cohesion<sup>41</sup>. The intriguing point is that remnants of these propagating modes are also present in the disordered (paramagnetic) phase of non-dissipative magnetic materials, provided that  $k\xi \sim 1$  (ref. 44); such spin-wave remnants describe the propagation of a signal within a correlated region of size  $\xi$ . It is possible that a similar phenomenon occurs in swarms: we find evidence of non-dissipative propagating modes in the correlation of the velocities,  $\mathbf{v}_i$ , which are directional degrees of freedom similar to the phase in magnetic materials; a strongly correlated swarm is therefore similar to a paramagnet with large correlation length. Within this physical context, the remnants of non-dissipative modes that we observe may be functional to propagate a coherent change of direction within the correlated regions the swarm is composed of.

We found non-dissipative modes in the region  $k\xi \sim 1$ . It would therefore be natural to expect hydrodynamics to take over and the correlation function to become exponential if we examined the regime  $k\xi \ll 1$ . Interestingly, in natural swarms this is impossible. Swarms are characterized by near-critical, scale-free spatial correlations, with a correlation length that scales with the system's size,  $\xi \sim L$  (ref. 22). To access the hydrodynamic region we would

therefore need  $k \ll 1/L$ , while the smallest accessible value is  $k \sim 1/L$ . We conclude that natural swarms are subject to a near-critical censorship of hydrodynamics. Several biological systems are believed to live in a near-critical regime<sup>45</sup> and may therefore share this same weird condition. This scenario makes dynamic scaling particularly relevant for strongly correlated biological systems: by generalizing to non-equilibrium phenomena the usual scaling laws, dynamic scaling is not restricted to the hydrodynamic regime and can thus make predictions that fall outside the long-wavelength region, yet enjoy a high degree of universality even in finite-size near-critical systems<sup>26</sup>. In particular, the dynamic critical exponent  $z$  is independent of the specific regime of  $k\xi$  and the dynamic universality class is therefore unequivocally identified. In natural swarms,  $z \approx 1$  and the existence of non-dissipative modes are hard experimental results any future theory must confront. Dynamic scaling may set equally useful benchmarks in other biological systems.

## Methods

Methods, including statements of data availability and any associated accession codes and references, are available in the [online version of this paper](#).

Received 25 November 2016; accepted 27 April 2017;  
published online 19 June 2017

## References

1. Widom, B. Equation of state in the neighborhood of the critical point. *J. Chem. Phys.* **43**, 3898–3905 (1965).
2. Kadanoff, L. The introduction of the idea that exponents could be derived from real-space scaling arguments. *Physics* **2**, 263–273 (1966).
3. Ferrell, R. A., Menyhard, N., Schmidt, H., Schwabl, F. & Szépfalusy, P. Dispersion in second sound and anomalous heat conduction at the lambda point of liquid helium. *Phys. Rev. Lett.* **18**, 891–894 (1967).
4. Halperin, B. I. & Hohenberg, P. C. Generalization of scaling laws to dynamical properties of a system near its critical point. *Phys. Rev. Lett.* **19**, 700–703 (1967).
5. Wilson, K. G. Renormalization group and critical phenomena. I. Renormalization group and the Kadanoff scaling picture. *Phys. Rev. B* **4**, 3174–3183 (1971).
6. Wilson, K. G. Renormalization group and strong interactions. *Phys. Rev. D* **3**, 1818–1846 (1971).
7. Attanasi, A. *et al.* Collective behaviour without collective order in wild swarms of midges. *PLoS Comput. Biol.* **10**, e1003697 (2014).
8. Cavagna, A. *et al.* Scale-free correlations in starling flocks. *Proc. Natl Acad. Sci. USA* **107**, 11865–11870 (2010).
9. Strandburg-Peshkin, A. *et al.* Visual sensory networks and effective information transfer in animal groups. *Curr. Biol.* **23**, R709–R711 (2013).
10. Ginelli, F. *et al.* Intermittent collective dynamics emerge from conflicting imperatives in sheep herds. *Proc. Natl Acad. Sci. USA* **112**, 12729–12734 (2015).
11. Dombrowski, C., Cisneros, L., Chatkaew, S., Goldstein, R. E. & Kessler, J. O. Self-concentration and large-scale coherence in bacterial dynamics. *Phys. Rev. Lett.* **93**, 098103 (2004).
12. Zhang, H.-P., Beer, A., Florin, E.-L. & Swinney, H. L. Collective motion and density fluctuations in bacterial colonies. *Proc. Natl Acad. Sci. USA* **107**, 13626–13630 (2010).
13. Tang, Q.-Y., Zhang, Y.-Y., Wang, J., Wang, W. & Chialvo, D. R. Critical fluctuations in the native state of proteins. *Phys. Rev. Lett.* **118**, 088102 (2017).
14. Attanasi, A. *et al.* Greta—a novel global and recursive tracking algorithm in three dimensions. *IEEE Trans. Pattern Anal. Mach. Intell.* **37**, 2451–2463 (2015).
15. Okubo, A., Bray, D. & Chiang, H. Use of shadows for studying the three-dimensional structure of insect swarms. *Ann. Entomol. Soc. Am.* **74**, 48–50 (1981).
16. Gibson, G. Swarming behaviour of the mosquito *Culex pipiens quinquefasciatus*: a quantitative analysis. *Physiol. Entomol.* **10**, 283–296 (1985).
17. Ikawa, T., Okabe, H., Mori, T., Urabe, K.-i. & Ikeshoji, T. A method for reconstructing three-dimensional positions of swarming mosquitoes. *J. Insect Behav.* **7**, 237–248 (1994).
18. Kelley, D. H. & Ouellette, N. T. Emergent dynamics of laboratory insect swarms. *Sci. Rep.* **3**, 1073 (2013).
19. Puckett, J. G., Kelley, D. H. & Ouellette, N. T. Searching for effective forces in laboratory insect swarms. *Sci. Rep.* **4**, 4766 (2014).
20. Butail, S. *et al.* 3D tracking of mating events in wild swarms of the malaria mosquito *Anopheles gambiae*. 2011 Annual International Conference of the IEEE Engineering in Medicine and Biology Society 720–723 (IEEE, 2011).
21. Butail, S. *et al.* Reconstructing the flight kinematics of swarming and mating in wild mosquitoes. *J. R. Soc. Interface* **9**, 2624–2638 (2012).
22. Attanasi, A. *et al.* Finite-size scaling as a way to probe near-criticality in natural swarms. *Phys. Rev. Lett.* **113**, 238102 (2014).
23. Puckett, J. G., Ni, R. & Ouellette, N. T. Time-frequency analysis reveals pairwise interactions in insect swarms. *Phys. Rev. Lett.* **114**, 258103 (2015).
24. Ni, R., Puckett, J. G., Dufresne, E. R. & Ouellette, N. T. Intrinsic fluctuations and driven response of insect swarms. *Phys. Rev. Lett.* **115**, 118104 (2015).
25. Ferrell, R., Menyhard, N., Schmidt, H., Schwabl, F. & Szépfalusy, P. Fluctuations and lambda phase transition in liquid helium. *Ann. Phys.* **47**, 565–613 (1968).
26. Halperin, B. I. & Hohenberg, P. C. Scaling laws for dynamic critical phenomena. *Phys. Rev.* **177**, 952–971 (1969).
27. Hohenberg, P. C. & Halperin, B. I. Theory of dynamic critical phenomena. *Rev. Mod. Phys.* **49**, 435–479 (1977).
28. Kibble, T. W. Topology of cosmic domains and strings. *J. Phys. A: Math. Gen.* **9**, 1387–1398 (1976).
29. Zurek, W. H. Cosmological experiments in superfluid helium? *Nature* **317**, 505–508 (1985).
30. Vicsek, T., Czirók, A., Ben-Jacob, E., Cohen, I. & Shochet, O. Novel type of phase transition in a system of self-driven particles. *Phys. Rev. Lett.* **75**, 1226–1229 (1995).
31. Grégoire, G. & Chaté, H. Onset of collective and cohesive motion. *Phys. Rev. Lett.* **92**, 025702 (2004).
32. Baglietto, G. & Albano, E. V. Finite-size scaling analysis and dynamic study of the critical behavior of a model for the collective displacement of self-driven individuals. *Phys. Rev. E* **78**, 021125 (2008).
33. Baglietto, G. & Albano, E. V. Nature of the order-disorder transition in the Vicsek model for the collective motion of self-propelled particles. *Phys. Rev. E* **80**, 050103 (2009).
34. Couzin, I. D., Krause, J., James, R., Ruxton, G. D. & Franks, N. R. Collective memory and spatial sorting in animal groups. *J. Theor. Biol.* **218**, 1–11 (2002).
35. Chaté, H., Ginelli, F., Grégoire, G., Peruani, F. & Raynaud, F. Modeling collective motion: variations on the Vicsek model. *Eur. Phys. J. B* **64**, 451–456 (2008).
36. Toner, J. & Tu, Y. Long-range order in a two-dimensional dynamical xy model: how birds fly together. *Phys. Rev. Lett.* **75**, 4326–4329 (1995).
37. Toner, J. & Tu, Y. Flocks, herds, and schools: a quantitative theory of flocking. *Phys. Rev. E* **58**, 4828–4858 (1998).
38. Kyriakopoulos, N., Ginelli, F. & Toner, J. Leading birds by their beaks: the response of flocks to external perturbations. *New J. Phys.* **18**, 073039 (2016).
39. Forster, D. Hydrodynamic fluctuations, broken symmetry, and correlation functions. *Frontiers in Physics* Vol. 47, 343 (WA Benjamin, Inc., 1975).
40. Chaikin, P. & Lubensky, T. *Principles of Condensed Matter Physics* (Cambridge Univ. Press, 2000).
41. Attanasi, A. *et al.* Information transfer and behavioural inertia in starling flocks. *Nat. Phys.* **10**, 691–696 (2014).
42. Gorboson, D. *et al.* Long-range acoustic interactions in insect swarms: an adaptive gravity model. *New J. Phys.* **18**, 073042 (2016).
43. Marshall, W. Critical scattering of neutrons by ferromagnets. *Natl. Bur. Std. (U. S.) Misc. Publ.* **273**, 135–142 (1966).
44. Marshall, W. & Lowde, R. Magnetic correlations and neutron scattering. *Rep. Prog. Phys.* **31**, 705–775 (1968).
45. Mora, T. & Bialek, W. Are biological systems poised at criticality? *J. Stat. Phys.* **144**, 268–302 (2011).

## Acknowledgements

We thank S. Caprara, F. Cecconi, F. Ginelli and J. G. Lorenzana for important discussions. This work was supported by IIT-Seed Artswarm, European Research Council Starting Grant 257126, US Air Force Office of Scientific Research Grant FA95501010250 (through the University of Maryland) and ERANET-LAC grant CRIB. T.S.G. was supported by grants from CONICET, ANPCyT and UNLP (Argentina).

## Author contributions

A.C. and I.G. designed the study. S.M. coordinated the experiment. C.C., L.D.C. and S.M. performed the experiment. L.P. and S.M. adapted the tracking algorithm and produced the 3D trajectories. S.M. and D.C. calculated the experimental correlation functions. T.S.G. wrote the code and ran the numerical simulations. A.C., D.C., I.G., T.S.G., S.M. and M.V. performed the theoretical analysis. A.C. wrote the paper.

## Additional information

Supplementary information is available in the [online version of the paper](#). Reprints and permissions information is available online at [www.nature.com/reprints](http://www.nature.com/reprints). Publisher's note: Springer Nature remains neutral with regard to jurisdictional claims in published maps and institutional affiliations. Correspondence and requests for materials should be addressed to A.C. or S.M.

## Competing financial interests

The authors declare no competing financial interests.

## Methods

**Experiments.** Data were collected in the field between May and October, in 2011, 2012 and 2015. We acquired video sequences using a multi-camera system of three synchronized cameras (IDT-M5) shooting at 170 fps. We used Schneider Xenoplan 50 mm  $f = 2.0$  lenses. Typical exposure parameters: aperture  $f = 5.6$ , exposure time 3 ms. Recorded events have a time duration between 1.5 and 15.8 s (see Supplementary Table 1). More details can be found in ref. 7. To reconstruct the 3D positions and velocities of individual midges we used the tracking method described in ref. 14. Our tracking method is accurate even on large moving groups and produces very low time fragmentation and very few identity switches, therefore allowing for accurate measurements of time-dependent correlations.

**Correlation function.** We define the dimensionless velocity fluctuations as

$$\delta \hat{\mathbf{v}}_i \equiv \frac{\delta \mathbf{v}_i}{\sqrt{\frac{1}{N} \sum_k \delta \mathbf{v}_k \cdot \delta \mathbf{v}_k}} \quad (8)$$

where  $\delta \mathbf{v}_i \equiv \mathbf{v}_i - \mathbf{V}$  and  $\mathbf{V}$  is the collective velocity of the swarm that takes into account global translation, rotation and dilation modes (see ref. 22). The spatio-temporal correlation function is the time generalization of the static space correlation function previously studied in refs 7,8,22,

$$C(r, t) = \left\langle \frac{\sum_{ij} \delta \hat{\mathbf{v}}_i(t_0) \cdot \delta \hat{\mathbf{v}}_j(t_0 + t) \delta[r - r_{ij}(t_0, t)]}{\sum_{ij} \delta[r - r_{ij}(t_0, t)]} \right\rangle_{t_0}$$

where  $r_{ij}(t, t) = |\mathbf{r}_i(t) - \mathbf{r}_j(t)|$  and the positions are calculated with respect to the centre of mass of the swarm, that is,  $\mathbf{r}_i(t_0) = \mathbf{R}_i(t_0) - \mathbf{R}_{CM}(t_0)$ ; the brackets indicate an average over time,

$$\langle f(t_0, t) \rangle_{t_0} = \frac{1}{t_{\max} - t} \sum_{t_0=1}^{t_{\max}-t} f(t_0, t) \quad (9)$$

where  $t_{\max}$  is the total available time in the simulation or in the experiment. The purpose of  $C(r, t)$  is to measure how much a change of velocity of an individual at time  $t_0$  influences a change of velocity of another individual at distance  $r$  at a later time  $t_0 + t$ . The (dimensionless) correlation function in Fourier space is given by

$$C(k, t) = \rho \int d\mathbf{r} e^{i\mathbf{k} \cdot \mathbf{r}} C(r, t) \quad (10)$$

By using the definition of  $C(r, t)$  and the approximation  $\sum_{ij} \delta[r - r_{ij}(t_0, t)] \sim 4\pi r^2 \rho N$  in the integral, we obtain

$$\begin{aligned} C(k, t) &= \left\langle \frac{1}{N} \sum_{ij} \int_{-1}^{+1} d(\cos\theta) e^{ikr_{ij} \cos(\theta)} \delta \hat{\mathbf{v}}_i \cdot \delta \hat{\mathbf{v}}_j \right\rangle_{t_0} \\ &= \left\langle \frac{1}{N} \sum_{ij} \frac{\sin(kr_{ij}(t_0, t))}{kr_{ij}(t_0, t)} \delta \hat{\mathbf{v}}_i \cdot \delta \hat{\mathbf{v}}_j \right\rangle_{t_0} \end{aligned} \quad (11)$$

which is the correlation function that we compute experimentally in the present work. Notice that, by definition,  $\sum_i \delta \hat{\mathbf{v}}_i = 0$ ; due to this sum rule we obtain  $C(k=0, t) = 0$ . The smallest non-trivial value of the wavenumber we can evaluate the correlation at is therefore  $k = 2\pi/L$ .

**Characteristic timescale  $\tau$ .** To compute the characteristic timescale  $\tau_k$ , we follow the classical definition of ref. 26 (see Supplementary Appendix A):

$$\int_0^\infty \frac{dt}{t} \sin(t/\tau_k) \hat{C}(k, t) = \pi/4 \quad (12)$$

For a purely exponential correlation,  $\tau_k$  coincides with the exponential decay time, while for more complex functional forms,  $\tau_k$  is the most relevant timescale of the system. Relation (12) gives an estimate of  $\tau_k$  that is more robust than simply crossing  $\hat{C}(k, t)$  with a constant and more reliable than a fit, as it does not require a priori knowledge of the functional form of  $\hat{C}(k, t)$ . Dealing with real data, we numerically solve:

$$\sum_{t=0}^T \frac{1}{t} \sin(t/\tau_k) \hat{C}(k, t) = \frac{\pi}{4} \quad (13)$$

where  $T$  is the time duration of the event of interest.

**Correlation length.** To compute the correlation length,  $\xi$ , we can directly work in  $k$  space. The static correlation function,  $C_0(k) \equiv C(k, t=0)$ , is

$$C_0(k) = \left\langle \frac{1}{N} \sum_{ij} \frac{\sin(kr_{ij})}{kr_{ij}} \delta \hat{\mathbf{v}}_i \cdot \delta \hat{\mathbf{v}}_j \right\rangle_{t_0} \quad (14)$$

where now both  $i$  and  $j$  are evaluated at equal time,  $t_0$ . By decreasing  $k$  we are averaging over larger length scales, therefore adding to (14) more correlated pairs, making  $C_0(k)$  increase. When the wavenumber arrives at  $k \sim 1/\xi$ , we start adding uncorrelated pairs; hence,  $C_0(k)$  must level. If we further decrease  $k$  and reach  $1/L$  (where  $L$  is the system's size) we start to be affected by the sum rule,  $C_0(k=0) = 0$ ; hence, the static correlation  $C_0(k)$  decreases, until eventually it vanishes for  $k=0$  (ref. 46). In a system where  $\xi \ll L$  the static correlation therefore has—in log scale—a broad plateau between  $k \sim 1/\xi$  and  $k \sim 1/L$ . However, natural swarms are scale-free systems, where  $\xi \sim L$  (ref. 22); in this case,  $C_0(k)$  has a well-defined maximum at  $k_{\max} \sim 1/\xi \sim 1/L$ . This is a very practical way to evaluate  $\xi$  if one is already working in  $k$  space and it is the one we use in this work. Alternatively, one can define  $\xi$  as the point where the static correlation in  $r$  space  $C_0(r) = C(r, t=0)$  reaches zero,  $C_0(r=\xi) = 0$ , as previously done in refs 7,8,22. These two definitions of  $\xi$  are consistent with each other (Supplementary Fig. 1) and they both give the same dynamic scaling results.

**Critical exponent.** The determination of the critical exponent,  $z$ , through the fit of equation (4) is quite tricky because the range of the experimental times,  $\tau_k$ , and lengths,  $\xi$ , is rather limited and data are noisy. We checked the reliability of the exponent found by the fit, comparing its value with the one that produces the best collapse of the correlation functions when rescaled by  $k^z t$ , equation (5). This last procedure is less affected by experimental noise than the fit of equation (4) since it does not need the computation of  $\tau_k$ , but it is not suitable to estimate the critical exponent of large data sets, because it may be hard to judge the quality of the collapse when rescaling a high number of correlation functions.

In Supplementary Fig. 2 we present the correlation functions' collapse obtained for  $z=2$ ,  $z=1$  and  $z=1.2$ . The figure clearly shows that the correlation functions rescaled by  $k^z t$  with  $z$  equal to 2 (Supplementary Fig. 2a) do not collapse on the same curve, while this happens for  $z=1$  (Supplementary Fig. 2b), confirming that the critical exponent is closer to 1 than to 2. Moreover, Supplementary Fig. 2c shows the best collapse by eye of the correlation functions, which occurs for  $z=1.2$  accordingly to the exponent obtained through the fit of equation (4).

**Simulations.** We simulated the Vicsek model<sup>30</sup> in three dimensions as in ref. 22. The updated equations are

$$\mathbf{v}_i(t+1) = v_0 \mathcal{R}_\eta \left[ \sum_{j \in S_i} \mathbf{v}_j(t) \right] \quad (15)$$

$$\mathbf{r}_i(t+1) = \mathbf{r}_i(t) + \mathbf{v}_i(t+1) \quad (16)$$

where  $S_i$  is a sphere of radius  $r_c$  centred at  $\mathbf{r}_i(t)$  and the operator  $\mathcal{R}_\eta$  normalizes its argument and rotates it randomly within a spherical cone centred at it and spanning a solid angle  $4\pi\eta$ . We chose  $\eta=0.45$ ,  $v_0=0.05$ ,  $r_c=1$ .

We considered systems of  $N=128, 256, 512, 1,024$  and  $2,048$  particles, a range consistent with the typical sizes of natural swarms. Dynamic scaling applies when  $\xi$  is large, so we chose to have the largest possible  $\xi$ , that is, to be at criticality. This makes sense also because natural swarms are near-critical systems<sup>22</sup>. To mimic the experimental situation, we fix the noise  $\eta$  and use  $x=r_1/r_c$  as control parameter, where  $r_1$  is the mean first-neighbour distance. Scaling is then tested at pairs of values  $(x, N)$  that lie along the critical line in the  $x, N$  plane. Note that  $r_1$  cannot be fixed a priori, but has to be determined from a simulation at a fixed average density.

For each value of  $N$ , several box sizes  $L$  were chosen to obtain different average densities. Five samples with random initial conditions were generated for each  $N$  and  $L$ . We ran each sample for  $10^5$  steps for equilibration and used a further  $5 \times 10^5$  steps for data collection. We verified that the polarization  $\Phi = (1/N) \sum_i \mathbf{v}_i / v_0$  remained stationary after the equilibration run, and that its correlation time was much shorter than  $10^5$ . We then determined  $r_1$  and computed the static correlation  $C(k, t=0)$ . This function has a maximum  $C_{\max}$  for some  $k \equiv k_{\max}$ .  $C_{\max}$  is a measure of the susceptibility  $\chi$  (in statistical physics  $\chi$  is given by the volume integral of  $C(\mathbf{r}, t=0)$ , but in our case this integral is 0 because of the fact that  $\sum_i \delta \mathbf{v}_i = 0$  (ref. 46)). We thus obtained  $\chi$  versus  $x$  curves from which we found the value of  $x$  that maximizes the susceptibility,  $x_c(N)$ : this is the finite-size critical point where the correlation length  $\xi$  is of order  $L$ . We finally computed  $C(k, t)$  at  $x_c(N)$  (averaging over all samples) at  $k=k_{\max}(x_c(N)) \sim 1/L$ . Since  $\xi \sim L$ , this fulfils the dynamic scaling condition  $k\xi = \text{const}$  that we also adopt in natural swarms.

**Data availability.** The data that support the plots within this paper and other findings of this study are available from the corresponding author on request.

## References

46. Cavagna, A. *et al.* Spatio-temporal correlations in models of collective motion ruled by different dynamical laws. *Phys. Biol.* **13**, 065001 (2016).